X-ray Combined QTA using a CPS applied to a ferroelectric ultrastructure

M. Morales [1], D. Chateigner [2], L. Lutterotti [3], J. Ricote [4]

[1] Lab. Physique de l'Etat Condensé, Univ. du Maine, BP 535, F-72085 Le Mans
[2] Lab. CRIStallographie et sciences des MATériaux-ISMRA, F-14050 Caen
[3] Dipartimento di Ingegneria dei Materiali, Univ. Di Trento, I-38050 Trento
[4] Instituto de Ciencia de Materiales de Madrid, CSIC, Cantoblanco, S-28049 Madrid

Keywords: Texture; Structure; X-Ray diffraction combined approach; Ferroelectric thin films; Modified lead titanates;

Abstract. The new combined methodology for quantitative description of texture, structure and other microstructural parameters of thin layers using X-ray diffraction is presented and applied to the case of a ferroelectric thin film of $Pb_{0.76}Ca_{0.24}TiO_3$ on a $Pt/TiO_2/SiO_2/Si$ substrate. The approach allows the quantitative texture analysis of the ferroelectric thin film and the Pt electrode, refining simultaneously their structure, layers thickness, mean crystallite size and microstrain state. The layer thickness determination is estimated by the refinement of the thicknesses inserted in the absorption and volumic correction factors. The powerfulness of this methodology is discussed and compared with other approaches.

Introduction

The microstructure of ferroelectric thin films is a determinant factor of their final properties, which are used in a wide range of technological applications [1,2]. Different techniques are used for this characterisation, and among them, X-ray diffraction has been routinely used as a non-destructive characterisation of texture, strain state, particle size, crystallographic structures, ... However, when applied to anisotropic polycrystalline samples, the classical diffraction approaches generally fail. For instance, a usual Bragg-Brentano diffraction diagram may not reveal all diffracted lines of a compound when it is strongly textured, making its structural determination impossible, and at the same time preventing any quantitative texture analysis. Also, strongly overlapping peaks often prevent any textural characterisation. This is usually the case of ferroelectric single thin films, and the situation becomes worth when bottom electrodes, anti-diffusion barrier or in general film stacking are used.

In this work, we have chosen the relatively recently developed approach [3], the so-called combined approach, which is able to determine all the parameters accessible by X-ray diffraction through the combination of adequate refinement procedures. We demonstrate that this approach allows the study of layered multiphase complex compounds. As an example, we apply it to a $Pb_{0.76}Ca_{0.24}TiO_3/Pt/TiO_2/SiO_2/Si(100)$ ultrastructure.

Materials and experimental procedure

A thin film of Ca-modified lead titanate of the nominal composition $Pb_{0.76}Ca_{0.24}TiO_3$ (PTC), was obtained by spin-coating deposition of a sol-gel processed solution [4] on a $Pt/TiO_2/SiO_2/Si(100)$

substrate previously treated at 650ºC during 30 min. The 4 layers deposited were crystallised layer-by-layer by rapid thermal processing (heating rate ~30ºC/s) at 650ºC for 50 s. Once the film is crystallised, a further thermal treatment at 650ºC during 1 hour is performed (heating rate 10ºC/min). The expected thickness of the PTC and Pt layers were approximately 400 nm and 50 nm respectively, as determined from the deposition parameters.

X-ray measurements were carried out with a Huber four-circle goniometer mounted on an X-ray generator equipped with a curved position sensitive detector (INEL CPS-120), as detailed elsewhere [5]. Spin-coated films usually exhibit fibre textures [5,6], which means that intensities are varying only with the tilt χ of the goniometer. Therefore, we summed all diagrams in φ for identical χ angles (11 resulting diagrams), in order to first refine background, 2θ offset, instrumental broadenings and defocusing effects. All calibrations for instrumental contributions were operated on a KCl powder measured in the same conditions. The nominal composition for the PTC layer was used in the refinement, starting with bulk-like cell parameters. A first cycle applied to all the diagrams extracted the integrated intensities using the Le Bail algorithm [7]. These intensities are used for a first refinement of the orientation distribution (OD) by the WIMV [8] or the entropy modified WIMV (E-WIMV) [9] iterative methods. The OD obtained is then introduced in the cyclic Rietveld refinement of the diagrams. The new refined parameters are used for a new WIMV cycle to obtain a new OD, and so on. In this way, the OD refinement takes progressively account of the microstructural and structural reality, while the Rietveld analysis is corrected for texture in a physically sound manner. All the necessary calculations were carried out in the MAUD package [10] in which the layered model for ultrastructures measurements using a curved detector was implemented [11]. The refinement quality is assessed by the comparison of the experimental and recalculated diagrams and by the reliability factors: RP for OD refinement, Rw and R_{Bragg} for Rietveld refinement.

Results and discussion

The experimental diagrams show a strong Pt preferred orientation with {111} parallel to the film plane (Fig. 1). The PTC film texture is difficult to analyse from θ-2θ spectra, because of the overlap between peaks of the ferroelectric film and the underlying substrate. This difficulty is furthermore enhanced because of the overlaps of the peaks from the PTC structure itself. Indeed, the PTC structure is a tetragonal perovskite, but with only few distortions of the perovskite cell, making it pseudo-cubic in reality. Hence 100 and 001 lines are located approximately at the same Bragg angles in the diagrams. Unfortunately, polarisation vectors are located for the analysed phase along the c-axes of the structure only, and it becomes crucial to be able to separate 100 from 001 textural contributions quantitatively.

Up to now, the direct integration method used [5,6] extracts the texture information of the thin film only from those peaks not influenced by the underlying layers of the substrate, reducing considerably the input data used in the OD refinement. In this case, the structural data used for the OD calculations correspond to ceramic materials of equivalent compositions, with crystals not growing with substrate-imposed restrictions. Therefore, the correct quantitative texture analysis of both phases can only be calculated using the combination of the Rietveld and WIMV-like algorithms. Figure 1 shows two refinement results for the diagrams measured at $\chi = 0°$ using the WIMV and E-WIMV algorithms. For the Rietveld simulation we have chosen atomic positions and isotropic thermal parameters as the ones of the bulk materials. Trying to free atomic coordinates during the refinement of the texture and microstructure always gave divergence of the program, probably because of an unsufficient number of experimental data compared to the number of fit parameters.

One can directly see the better refinement obtained using the E-WIMV approach, particularly for the very sharp peaks of Pt, which already denotes a strong texture, and of the ones corresponding to the Si single crystal. Note that we are able with this procedure to perform a reliable analysis of the Pt layer, which is covered by the ferroelectric thin film, thanks to the layer model implemented in the calculations. The layer model implemented for our calculations is based on the correction factors used to correct data for absorption and volume variations, for the PTC film [12]:

$$C_{\chi}^{\text{top film}} = g_1\left(1-\exp\left(-\mu T g_2/\cos\chi\right)\right)/\left(1-\exp\left(-2\mu T/\sin\omega\cos\chi\right)\right),$$

and the Pt electrode:

$$C_{\chi}^{\text{cov. layer}} = C_{\chi}^{\text{top film}}\left(\exp\left(-g_2\sum\mu_i' T_i'/\cos\chi\right)\right)/\left(\exp\left(-2\sum\mu_i' T_i'/\sin\omega\cos\chi\right)\right)$$

in which equations ω is the incidence angle of x-rays, μ is the linear absorption coefficient of a film of thickness T which would be placed on the top of the stack, μ_i' is the linear absorption coefficient of the films of thickness T_i' that would cover a bottom layer, g_1 and g_2 are geometrical factors taking account of the experimental set-up and of the peak position on the detector.

Figure 2 shows a selected series of diagrams measured at increasing tilt angles (every 5°), with their corresponding refinements using the E-WIMV approach. All the diagrams are nicely reproduced, with reliability factors R_{Bragg} as low as 4.7 % (Tab. 1). The small observed discrepancies are due to strong substrate peak feet. From the refined orientation distribution we can recalculate the pole figures (Fig. 3), for the PTC and Pt layers.

The refinement was made on the 19 and 4 first available pole figures for PTC and Pt, respectively, but we present only the low-indices ones. In agreement with the diffraction diagrams, all the reliability factors indicated a better refinement using the E-WIMV approach (Tab. 1), which also indicated a stronger texture (higher texture indexes) both for PTC and Pt layers. This is due to the better ability of the E-WIMV algorithm to represent strong textures.

Texture indexes are 2 mrd^2 for PTC and 41 mrd^2 for Pt. While the Pt layer only shows preferential orientation along <111>, the ferroelectric PTC film has also a small component along <100> perpendicular to the film. Interestingly, no significant component along <001> is observed (Fig. 3). The results of the microstructural parameters (Tab. 2) reveal the presence of larger microstrains in the PTC films than in the Pt layer, which presents the largest mean crystallite size. This is consistent with the fact that crystallites of the PTC film have sizes not larger than one tenth of the total layer thickness, while the Pt layer exhibits a mean crystallite size which extends to the full thickness of the layer. The values obtained for the Pt and PTC layers thickness are very close to the ones expected from the deposition conditions.

	Pt Texture Index (m.r.d.^{2})	PTC Texture Index (m.r.d.^{2})	Pt RP_0 (%)	PTC RP_0 (%)	Rw (%)	R_{Bragg} (%)
WIMV	48.1	1.3	18.4	11.4	12.4	7.7
E-WIMV	40.8	2	13.7	11.2	7	4.7

Tab. 1: Texture indexes and Reliability factors for the refinement of the PTC ultrastructure

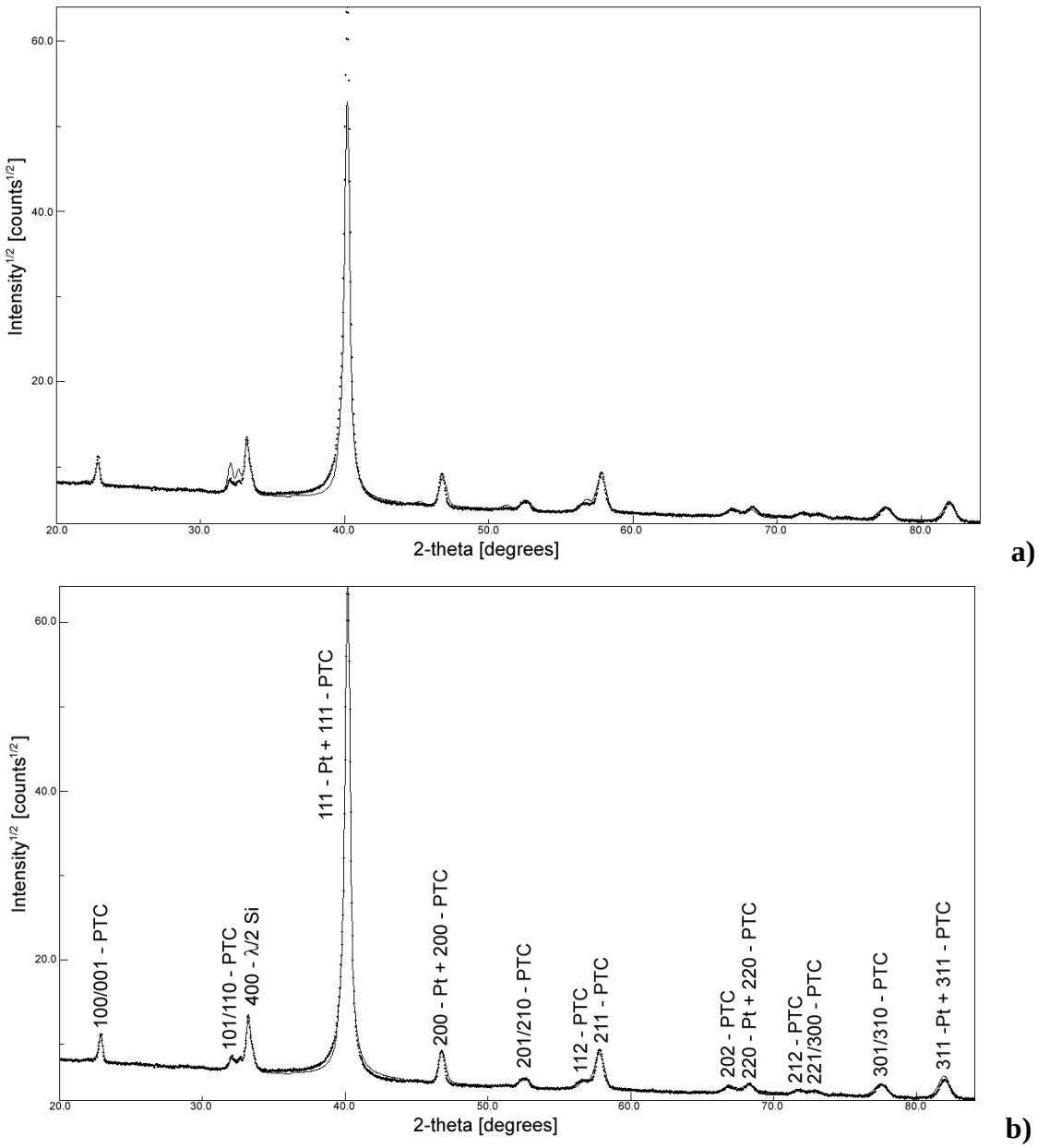

Fig. 1: Experimental (dotted line) and refined (solid line) diagrams for $\chi = 0^{o}$, using the WIMV **(a)** and E-WIMV **(b)** approaches.

	Cell parameters (Å)	Cryst. Size (Å)	μstrain param.	Layer thickness (Å)
Pt	3.955(1)	462(4)	0.0032(1)	458(3)
PTC	a=3.945(1) c=4.080(1)	390(7)	0.0067(1)	4080(1)

Tab. 2: Refined parameters for the PTC and Pt layers

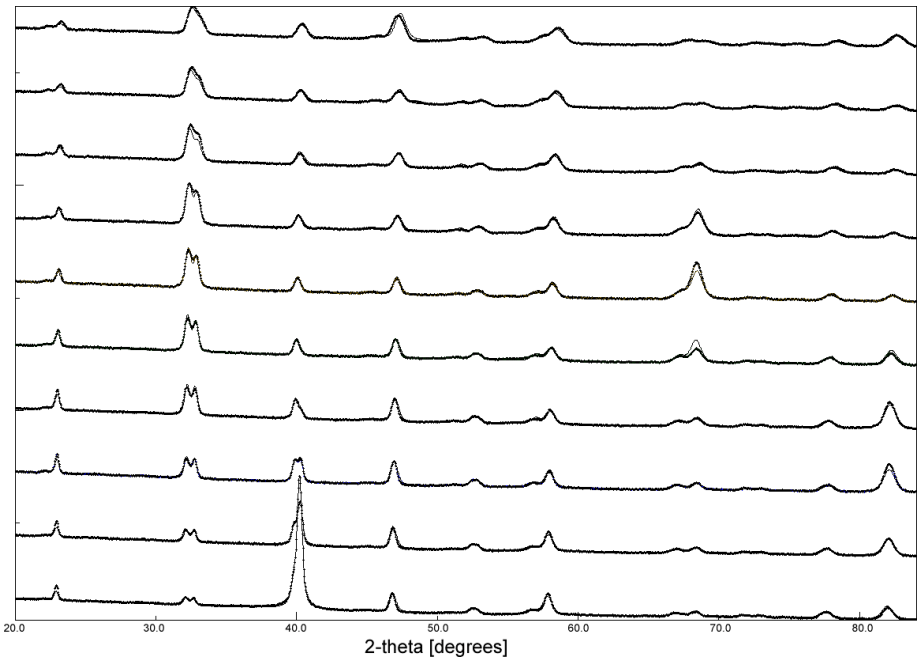

Fig. 2: Experimental (dotted line) and refined (solid line) diagrams from χ = 5° (bottom) to χ = 45° (top) step 5°, using E-WIMV combined with Rietveld analysis.

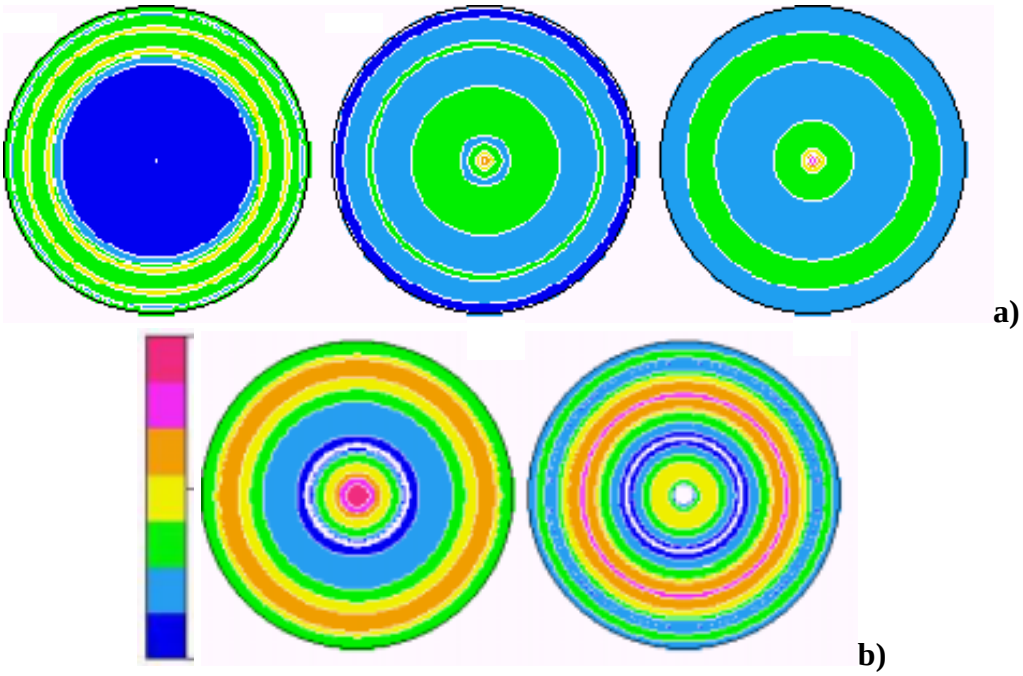

Fig. 3: Pole figures recalculated after E-WIMV refinement for **(a)** PTC: {001}, {100} and {111} pole figures from left to right (linear density scale, max = 3.8 m.r.d., min = 0.1 m.r.d.) and **(b)** Pt: {111} and {200} pole figures from left to right (logarithmic density scale, max = 63 m.r.d., min = 0) layers. Equal area projections.

Compared to previous studies [5,6], the approach appears to be much more powerful in extracting structural, microstructural and textural parameters in complex samples. Parameters divergence reveals to be astonishingly low, provided strongly dependent parameters were not released at the same time. This stability is very probably due to the high number of experimental pole figures taken into account in the refinements, allowing a decrease of the defocusing effect (large at high χ-ranges) and a reduction of the number of OD solutions.

In summary, we present in this paper a new methodology for the analysis of X-ray diffraction data. Up to now, it has not been possible to obtain simultaneously reliable results of texture, structure and other microstructural parameters. This method also allows the study of other layers like the Pt bottom electrode. Applied to a ferroelectric thin ultrastructures, we extract important information for the optimisation of the material in view of its application in devices, which will be the focus of further work.

Acknowledgements
This work has been funded by EU project GROWTH (G6RD-CT99-00169).

References

[1] J. F. Scott, Ferroelectric Memories, Springer Series in Advanced Microelectronics 3, Springer-Verlag Berlin Heidelberg 2000.
[2] D.L. Polla and L.F. Francis, MRS Bull. **21[7]**, 59-65 (1996).
[3] M. Ferrari, L. Lutterotti, J. Appl. Phys. **76(11)**, 7246-7255 (1994).
[4] R. Sirera and M.L. Calzada, Mat. Res. Bull. **30[1],** 11-18 (1995).
[5] J. Ricote, D. Chateigner Bol. Soc. Esp. Cerám. y Vidrio, **38[6]**, 587-591 (1999).
[6] J. Ricote, D. Chateigner, L. Pardo, M. Algueró, J. Mendiola and M.L. Calzada, Ferroelectrics **241,** 167-174 (2000).
[7] A. Le Bail, H. Duroy, J.-L. Fourquet, Mater. Res. Bull. **23**, 447-452 (1988).
[8] S. Matthies and G.W. Vinel, Phys. Stat. Sol. B **112**, K111-K120 (1982).
[9] L. Yansheng, W. Fu, X. Jiazheng, L. Zhide, J. Appl. Cryst. **26**, 268-271 (1993).
[10] L. Lutterotti, S. Matthies, H.-R. Wenk in "Textures of Materials" vol 2, NRC Research Press J.A. Szpunar Ed., 1599-1604 (1999).
[11] A. Tizliouine, J. Bessières, J.-J. Heizmann, J.F. Bobo, Mat. Sci. For. **157**, 227-234 (1994).
[12] J.-J. Heizmann, C. Laruelle, J. of Appl. Cryst. **19**, 1986, 467-472.